

amplitudes, and there were somewhat larger delays for  $P(6)$  and the nondegenerate cases, respectively. The expected similarities between the models was explained earlier, and these calculations indeed show that in the absence of an independent way of determining  $\theta$ , there is no way to distinguish easily which case one is dealing with if observations are restricted to the region around the maximum delay.

## V. CONCLUSIONS

Some modifications of coherent pulse propagation in attenuating media which originate from degeneracy have been examined. It is found that the effect of SIT, first described by Hahn and McCall, is modified in an essential way. Among these modifications are the development of pulse shapes for large  $\theta$  which are characteristic of the degeneracy, the association of a finite loss with propagation, a reduction of delay times, and the suppression of pulse separation. Unfortunately, the latter three qualitatively tend to modify the propagation behavior in a manner similar to the introduction of a finite  $T_2$ . It also appears that, in the presence of attenuation, propagation can occur at constant angle

(fixed area attenuation). This implies considerable pulse broadening and resembles nondegenerate SIT, in accord with experimental findings. The resemblance is so close, that on the basis of transmission curves, delay curves, and pulse shapes alone is hard to distinguish between the two.

At high excitations [ $\theta(0) \gg \pi$ ] sufficiently degenerate media depart from the similarity to the nondegenerate case. A coherent saturation occurs which induces pulse sharpening. This type of behavior provides an essential distinction between degenerate and nondegenerate media. It can be understood without the additional complication of inhomogeneous broadening. Indeed, the influence of inhomogeneous broadening on the high-intensity behavior of a degenerate system can be regarded as arbitrarily small if the saturation width is sufficiently large.

## ACKNOWLEDGMENTS

We gratefully acknowledge the support and encouragement of Professor A. Javan throughout the entire term of this research. We also thank Professor Marlan O. Scully for his collaboration and continued interest.

## Analysis of Periodic Schottky Deviations

HENRY F. GRAY

Naval Research Laboratory, Washington, D. C. 20390

(Received 3 October 1969)

The theory of periodic Schottky deviations is studied numerically. Corrections to experimental surface reflection coefficients for several refractory metals are given. The corresponding corrected estimates of the surface inner potentials are in fair agreement with bulk band-theory calculations.

## I. INTRODUCTION

**A**N estimate of the electron inner potential of metals in the surface region and the confirmation of proposed shapes of the one-dimensional surface-potential barrier can be made by measuring the complex surface reflection coefficient  $\mu$  ( $\mu = |\mu| e^{i \arg \mu}$ ).<sup>1</sup> Reflection coefficients that have been obtained from an analysis of periodic deviations in the Schottky effect in thermionic emission from polycrystalline wires have been reported for several metals.<sup>2-4</sup> There are several approximate analytic expressions that describe the

periodic deviations.<sup>5,6</sup> However, the expression given by Miller and Good<sup>5</sup> has been favored more recently by experimentalists because the generalized WKB wave functions used by Miller and Good are more accurate for realistic one-dimensional barriers than the usual WKB wave functions.<sup>1,5,7</sup> Recent experimental results, though, have pointed out two discrepancies. First, if the Sommerfeld box model<sup>8</sup> of the surface potential is used to calculate reflection coefficients, it is necessary

<sup>5</sup> S. C. Miller, Jr., and R. H. Good, Jr., Phys. Rev. **92**, 1367 (1953).

<sup>6</sup> D. W. Juenker, G. S. Colladay, and E. A. Coomes, Phys. Rev. **90**, 772 (1953); D. W. Juenker, *ibid.* **99**, 1155 (1955); P. H. Cutler and J. J. Gibbons, *ibid.* **111**, 394 (1958).

<sup>7</sup> S. C. Miller, Jr., and R. H. Good, Jr., Phys. Rev. **91**, 174 (1953).

<sup>8</sup> The Sommerfeld box model of a metal is a one-dimensional surface potential model in which the metal's inner potential is a constant  $-W_a$ . This constant value joins the classical image motive just outside the metal surface. See Fig. 1 and Eq. (1) of Ref. 5, and footnote 9 of Ref. 2.

<sup>1</sup> C. Herring and M. H. Nichols, Rev. Mod. Phys. **21**, 185 (1949).

<sup>2</sup> I. J. D'Haenens and E. A. Coomes, Phys. Rev. Letters **17**, 516 (1966).

<sup>3</sup> R. E. Thomas and G. A. Haas, Phys. Rev. Letters **19**, 1117 (1967).

<sup>4</sup> W. C. Niehaus, in Proceedings of the Twenty-Ninth Annual Conference on Physical Electronics, Yale University, New Haven, Conn., 1969 (unpublished).

to assume values of the inner potential  $W_a$  as high as 24 eV for Mo and 28 eV for Re,<sup>2</sup> whereas band-structure calculations indicate values of only 12 eV<sup>9</sup> and 16 eV,<sup>10</sup> respectively. Furthermore, using the free-electron-gas model, such high values of  $W_a$  can only be explained by assuming that essentially all valence electrons should be treated as free. The second discrepancy is that the magnitude of the experimental surface reflection coefficient  $|\mu|$  is field-dependent.<sup>3,4</sup> The analytic expressions<sup>5,6</sup> describing the periodic deviations have been based on the assumption that  $\mu$  is essentially field-independent.

Because of the above two discrepancies and because of uncertainty in the accuracy of the least-squares data-reduction methods, a numerical study of the theory of periodic deviations in the Schottky effect was made in order to determine whether or not the discrepancies were real, or due to mathematical approximations in the theory<sup>5,7</sup> to model potentials, or to data-reduction techniques.

## II. CALCULATIONS

The following approach was used: A mock periodic deviations experiment was performed in which hypothetical thermionic current densities were numerically generated. Equation (1a) describes the thermionic electron-emission current density  $J(f)$  from a free-electron-gas model in which the electron transmission coefficient  $D(\epsilon, f)$  is a function of the energy  $\epsilon$  associated with the component of momentum normal to the surface.

$$J(f) = \frac{J_0}{kT} \int_{-w_a}^{\infty} D(\epsilon, f) e^{-\epsilon/kT} d\epsilon, \quad (1a)$$

where

$$J_0 = [4\pi m e (kT)^2 / h^3] e^{-e\phi/kT}, \quad (1b)$$

where  $k$  is the Boltzmann constant,  $h$  is Planck's constant,  $m$  and  $e$  are the free-electron mass and charge, respectively,  $\phi$  is the electron work function,  $T$  is the temperature in  $^{\circ}\text{K}$ ,  $f$  is the electrostatic field,  $\epsilon$  is the electron energy with respect to a zero at the barrier maximum for  $f=0$  (i.e.,  $x=\infty$ ), and  $W_a$  is the electron inner potential. Equation (1a) can be approximated to several significant figures by

$$j(f) = B \int_{\epsilon_1}^{2.1\text{eV}} D(\epsilon, f) e^{-\epsilon/kT} d\epsilon, \quad (1c)$$

where  $B$  is rather arbitrary in these calculations [see Eq. (5)] and the values of  $\epsilon=2.1$  eV and  $\epsilon=\epsilon_1$  were chosen as the upper and lower limits of integration, respectively, for the desired accuracy.

Since periodic deviations are an electron interference phenomenon, it is convenient to discuss the total

reflection  $[1-D(\epsilon, f)]$  in terms of two reflecting regions and to calculate each reflection coefficient separately. As was first suggested by Herring and Nichols<sup>1</sup> and later used in various theories,<sup>5,6</sup> the region of the metal surface itself and that of the barrier maximum can be characterized by the complex reflection coefficients  $\mu$  and  $\lambda$ , respectively. It was further assumed in these theories<sup>5,6</sup> that (1) these two reflecting regions are separated by a nonreflecting region that supports WKB wave functions, and (2) the electron reflection that occurs from the metal surface up to this WKB region is field-independent. In order to check numerically if such a nonreflecting region did, in fact, exist, and if it did exist, how far from the surface it extended, the following approach was used. For a given energy  $\epsilon$ , a purely ingoing plane wave was set up inside the metal. After choosing a value of the field  $f$ , the Schrödinger equation was numerically integrated out through the surface to some point  $X_j$  between the metal surface and the barrier maximum. The integrating method was similar to that described by Blatt<sup>11</sup> with special starting and stopping procedures. At the point  $X_j$  the reflection coefficient  $\mu(\epsilon, f)$  was calculated by joining the numerical solution to WKB wave functions. A nonreflecting region was determined when  $\mu(\epsilon, f)$  did not change appreciably as  $X_j$  was varied. As an additional check, the WKB criterion given by Eq. (3) below was used. The field independence was determined when  $\mu(\epsilon, f)$  did not change appreciably as the field  $f$  was varied from  $10^4$  to  $10^6$  V/cm. In the neighborhood of  $X_j=4$  Å, a nonreflecting region did exist that was essentially field-independent, in that

$$\frac{|\mu(\epsilon, f_2)| - |\mu(\epsilon, f_1)|}{|\mu(\epsilon, \bar{f})|} \leq 0.02, \quad (2)$$

where  $f \simeq 10^4$  V/cm,  $\bar{f} \simeq 10^5$  V/cm, and  $f_2 \simeq 10^6$  V/cm. For  $X_j > 4$  Å, the field dependence of the  $\mu$  reflection coefficient increased substantially with distance from the metal surface. Consequently, it can be concluded that if real surface potentials do not approach the classical image motive sufficiently well beyond  $X_j=4$  Å, the analytic expressions<sup>5,6</sup> describing periodic deviations should not be used in their present forms.

After the point  $X_j=4$  Å was chosen, the  $\lambda$  reflection coefficient was calculated in the following manner. For a given energy  $\epsilon$  and field  $f$ , a purely outgoing WKB wave function was set up at a point  $X_s$  greater than the barrier maximum. The point  $X_s$  was determined by requiring that at  $X_s$  the WKB criterion<sup>12</sup> be sufficiently well satisfied, i.e.,

$$|\hbar p' / p^2| [\frac{3}{4} - \frac{1}{2}(p p'' / p^2)]^{1/2} \simeq 10^{-4}, \quad (3)$$

where  $p$  is the normal momentum,  $h$  is Planck's con-

<sup>11</sup> J. C. Blatt, *J. Comput. Phys.* **1**, 382 (1967).

<sup>9</sup> T. L. Loucks, *Phys. Rev.* **139**, A1181 (1965). Also see T. L. Loucks, *ibid.* **143**, 506 (1966).

<sup>10</sup> L. F. Mattheiss, *Phys. Rev.* **151**, 450 (1966).

<sup>12</sup> J. L. Powell and B. Craseman, in *Quantum Mechanics* (Addison-Wesley Publishing Co., Inc., Reading, Mass., 1961), p. 142.

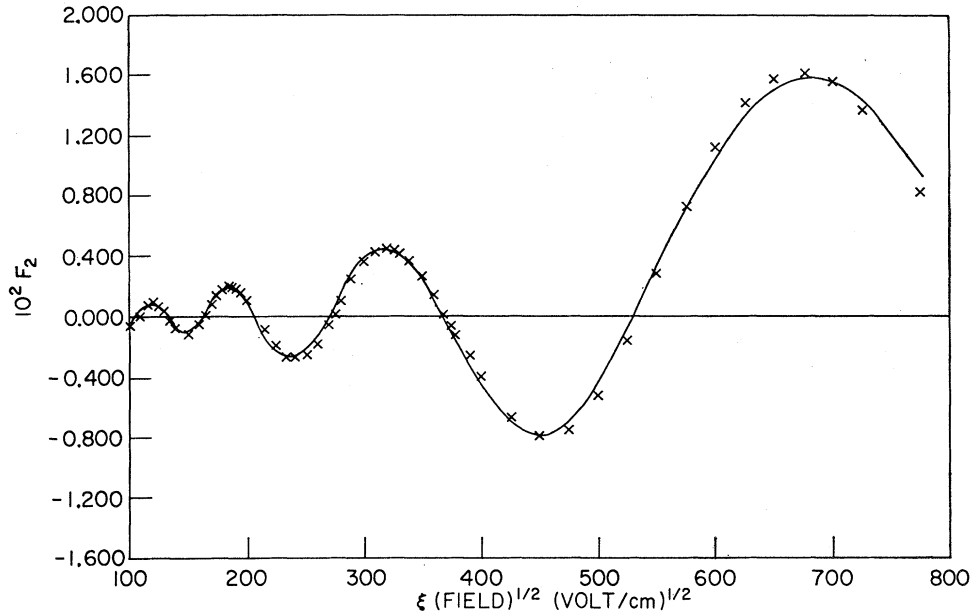


FIG. 1. Numerically generated periodic deviations from a Sommerfeld box metal with inner potential  $W_0 = 15$  eV and temperature  $T = 1500^\circ\text{K}$ . The "x" marks are the reduced data. The solid curve is the Miller-Good  $F_2$  term resulting from a least-squares fit to the data. The best-fit values of the surface reflection coefficient are  $|\mu| = 0.28$  and  $\arg\mu = -0.46$ .

stant, and the primes denote derivatives with respect to distance. ( $X_s$  varied from  $200 \text{ \AA}$  for  $f \geq 1.5 \times 10^5$  V/cm to  $400 \text{ \AA}$  for  $f \leq 5 \times 10^4$  V/cm.) The Schrödinger equation was then integrated to  $X_j = 4 \text{ \AA}$  (using as many as 7000 integration steps) where the reflection coefficient  $\lambda(\epsilon, f)$  was calculated using the same WKB wave functions at  $X_j$  that were used in the calculation of  $\mu(\epsilon, f)$ .

The total transmission coefficient  $D(\epsilon, f)$  was obtained by using the values of  $\mu$  and  $\lambda$  in the following relationship:

$$D(\epsilon, f) = \frac{(1 - |\lambda(\epsilon, f)|^2)(1 - |\mu(\epsilon, f)|^2)}{|1 - \mu(\epsilon, f)\lambda(\epsilon, f)|^2}. \quad (4)$$

The values of  $D(\epsilon, f)$  obtained using Eq. (4) were compared with several values of  $D(\epsilon, f)$  that were obtained by integrating the Schrödinger equation over the entire range of  $X$ . The values of  $D(\epsilon, f)$  obtained using both methods were the same (to about 10 significant figures).

Similar computer calculations of electron reflection coefficients for one-dimensional surface barriers have been conducted in the past by Cutler and Davis<sup>13</sup> and by Belford *et al.*<sup>14</sup> In neither of these studies was any attempt made to separate and analyze the effect of the surface region *per se* from the rest of the barrier, as is done in the theoretical treatments of periodic deviations.<sup>5,6</sup> Even though periodic deviations were not generated by Cutler and Davis,<sup>13</sup> good agreement exists

between their calculated total reflection coefficients and those calculated in this study.

Using the notation in Ref. 3, the Schottky curve should be of the form

$$\log_{10} j(\xi) = P + (Q/T)\xi + F(|\mu|, \arg\mu, \xi, T), \quad (5)$$

where  $P$ ,  $Q$ ,  $|\mu|$ , and  $\arg\mu$  are fitting constants,  $\xi = \sqrt{f}$  ( $f$  in V/cm), and  $T$  is the temperature in  $^\circ\text{K}$ .  $F$  describes the periodic Schottky deviations and it consists of a periodic term  $F_2$  and a monotonic term  $F_1$ . Although most investigators have used only the periodic term  $F_2$ , the addition of the monotonic term  $F_1$  could possibly affect the results because of its significant dependence on  $f$ . Therefore, in the mock experiment, the data-reduction method was performed both with the combined  $F_1 + F_2$  terms as well as the standard method using only the  $F_2$  term.

The expressions describing the  $F_1$  and  $F_2$  terms are

$$F_2 = (|\mu|/T)A(\xi) \sin[R(\xi) + \arg\mu], \quad (6)$$

$$F_1 = |\mu|^2 g(\xi) + h(\xi), \quad (7)$$

where

$$A(\xi) \simeq 1.3 \times 10^{-3} [C(\xi)^{3/2}] \xi^{7/4}, \quad (8)$$

$$C(\xi) \simeq 1.007(1 - 0.079 \ln \xi), \quad (9)$$

$$R(\xi) \simeq \frac{357.1}{\xi^{1/2}} + \frac{1}{2} \left[ \tan^{-1} C(\xi) + C(\xi) \ln \frac{4 + 4C(\xi)^2}{1 + 4C(\xi)^2} \right], \quad (10)$$

$$g(\xi) \simeq -0.434 \left[ 1 - (5.23 \times 10^{-3}/T) \xi^{3/2} \right], \quad (11)$$

$$h(\xi) \simeq (1.957/T^2) \xi^3. \quad (12)$$

<sup>13</sup> P. H. Cutler and J. C. Davis, *Surface Sci.* 1, 194 (1964).

<sup>14</sup> G. G. Belford, A. Kuppermann, and T. E. Phipps, *Phys. Rev.* 128, 524 (1962).

### III. RESULTS

Figure 1 is a plot of the numerically generated periodic deviations from a box-model<sup>8</sup> metal with a surface inner potential  $W_a = 15$  eV. The "x" marks are the reduced numerical data and the solid curve is the Miller-Good theory curve given by Eq. (6). The amplitude and argument of the surface reflection coefficient used in Eq. (6) were obtained by a least-squares fitting procedure using linear fitting parameters and the  $F_2$  term. These values are designated  $|\mu|_{\text{linear}}$  and  $\arg\mu_{\text{linear}}$ , respectively. (The  $F_1$  term was neglected here. Other methods are described later that use non-linear fitting parameters and include the  $F_1$  term.) It is seen that the field dependence of the numerically generated deviations (using the box model) is in good agreement with that described by Eq. (6). In particular, the anomalous rise in the deviation amplitude with field that was experimentally reported for real metals<sup>3,4</sup> is not observed. Consequently, this particular discrepancy between the Miller-Good theory and experimental behavior appears to lie in the surface-potential model used (i.e., the relative energy independence of the box model) rather than other mathematical approximations.

While the analytic expression [Eq. (6)] adequately describes the form of the deviations from a box-model metal, the amplitude and argument of  $\mu$  that must be used to fit the mock data do not agree with the anticipated values obtained from Miller and Good's analytic expression for  $\mu$  [Eq. (13)].

$$\mu_{\text{real}} \simeq (H_0^{(2)}(z) + iH_1^{(2)}(z)) / (-H_1^{(1)}(z) + iH_0^{(1)}(z)) \Big|_{z=(2W_a)^{-1/2}}, \quad (13)$$

where  $H_i^{(j)}(z)$  are Hankel functions and the inner potential  $W_a$  is expressed in Hartree units ( $\hbar = m = e = 1$ ).<sup>15</sup> In fact, the best fit values from Fig. 1 are  $|\mu|_{\text{linear}} = 0.28$  and  $\arg\mu_{\text{linear}} = -0.46$ , compared with the theoretical values (obtained from Eq. (13) using  $W_a = 15$  eV) of  $|\mu|_{\text{real}} = 0.22$  and  $\arg\mu_{\text{real}} = -0.19$ . Similar comparisons were made for box-model<sup>8</sup> metals with  $W_a = 10$  and 20 eV. The resultant corrections to the experimental surface reflection coefficients ( $|\mu|_{\text{linear}}$  and  $\arg\mu_{\text{linear}}$ ) that must be used to obtain the real values ( $|\mu|_{\text{real}}$  and  $\arg\mu_{\text{real}}$ ) are given by Eqs. (14):

$$|\mu|_{\text{real}} = \frac{3}{4} |\mu|_{\text{linear}} + 0.01, \quad (14a)$$

$$\arg\mu_{\text{real}} = \arg\mu_{\text{linear}} + 0.27 \text{ (rad)}. \quad (14b)$$

The experimental values of the surface reflection coefficient  $|\mu|$  recently reported<sup>3,4</sup> for several metals were corrected using Eq. (14a), and the corrected values were used in Eq. (13) to estimate the surface inner potentials  $W_a$ . The results, which are given in Table I, now show rather close agreement with bulk inner

<sup>15</sup> Numerical integration of the Schrödinger equation in the surface region for several values of  $W_a$  resulted in values of the reflection coefficient  $|\mu|$  substantially the same as that given by Eq. (13).

TABLE I. Corrected surface reflection coefficients and their corresponding inner potentials in the surface region for several refractory metals.

Metal	$ \mu _{\text{exp}}$	$(W_a)_{\text{uncorr}}^a$	$(W_a)_{\text{corr}}^a$	$(W_a)_{\text{calc}}$	$N_{\text{free}}^b$
Mo	0.26 <sup>c</sup>	22	11	12 <sup>d</sup>	1.2
Re	0.29 <sup>c</sup>	29	14	16 <sup>e</sup>	1.9
Ir	0.31 <sup>f</sup>	35	16	16 <sup>g</sup>	2.3
Ta	0.36 <sup>h</sup>	52	24	10 <sup>i</sup>	7.3
Nb	0.35 <sup>h</sup>	50	23	13 <sup>i</sup>	6.7

<sup>a</sup> See Eqs. (13) and (14).

<sup>b</sup> See Eq. (4), Ref. 2.

<sup>c</sup> See Table I, Ref. 2.

<sup>d</sup> Reference 9.

<sup>e</sup> Reference 10.

<sup>f</sup> Reference 3.

<sup>g</sup> See Table I, Ref. 16.

<sup>h</sup> Reference 4.

<sup>i</sup> L. F. Mattheiss (Private communication).

potentials obtained from band-theory calculations for Mo,<sup>9</sup> Re,<sup>10</sup> and Ir.<sup>16</sup> However, experimental results of Ta and Nb<sup>4</sup> still appear too high compared to some unpublished recent band-theory calculations.<sup>17</sup> Because the inner potential  $W_a$  is the sum of the Fermi energy  $E_F$  and the work function  $\phi$ , published work functions and the corrected  $W_a$ 's in Table I can be used to obtain an estimate of the Fermi energy  $E_F$ . Analyzing this in terms of the free-electron-gas model, the effective number of free electrons per atom ( $N_{\text{free}}$ ) in the surface region can be estimated. The values of  $N_{\text{free}}$  so obtained for the metals checked are tabulated in column 6 of Table I. It is to be noted that, contrary to the correlation suggested by D'Haenens and Coomes<sup>2</sup> and used by Smith,<sup>18</sup> these corrected values are not the same as their group numbers in the periodic table.

### IV. EXPERIMENTAL ANALYSIS PROCEDURES

While the least-squares data-reduction methods most often used to analyze periodic deviations have given equal weight to all experimental current densities, they have the inherent limitation that the relative error in  $F_2$  will appear larger at low fields since the amplitude of  $F_2$  increases with field. In order to give the same relative error to each period, the deviations data can be normalized with respect to temperature and amplitude as follows:

$$M(\xi) = [T/A(\xi)] [\log_{10} j(\xi) - P - (Q/T)\xi], \quad (15a)$$

where  $P$  and  $Q$  are the values of the fitting parameters obtained from the first step of the data-reduction analysis such as that described in Sec. III. These values of  $M(\xi)$  are then treated as new data that should have the form shown in Eq. (15b):

$$N(\xi) = |\mu|_{\text{norm}} \sin[R(\xi) + \arg\mu_{\text{norm}}]. \quad (15b)$$

Equation (15b) is least-squares fitted with linear fitting parameters to the values of  $M(\xi)$  given in Eq. (15a).

<sup>16</sup> O. K. Andersen and A. R. Mackintosh, Solid State Commun. **6**, 285 (1968).

<sup>17</sup> L. F. Mattheiss (private communication).

<sup>18</sup> J. R. Smith, Phys. Rev. **181**, 522 (1969).

$|\mu|_{\text{norm}}$  and  $\arg\mu_{\text{norm}}$  are then obtained from those linear fitting parameters. The resultant corrections to the normalized experimental surface reflection coefficients ( $|\mu|_{\text{norm}}$  and  $\arg\mu_{\text{norm}}$ ) that must be used to obtain the real values  $|\mu|_{\text{real}}$  and  $\arg\mu_{\text{real}}$  are given by Eqs. (16):

$$|\mu|_{\text{real}} = \frac{3}{4}|\mu|_{\text{norm}} + 0.02, \quad (16a)$$

$$\arg\mu_{\text{real}} = \arg\mu_{\text{norm}} + 0.13(\text{rad}). \quad (16b)$$

It is seen that the corrections necessary for the normalized values [Eq. (16)] are slightly less than those for the usual least-squares fitting values given in Eqs. (14). Furthermore, when the least-squares analysis with  $F_2$  was done with nonlinear fitting parameters and the usual one-step procedure (non-normalized), the magnitude of the surface reflection coefficient  $|\mu|$  was 15% greater than that obtained using linear fitting parameters. However, the magnitude of  $\mu$  obtained from the two-step procedure [using the normalized expression shown in Eq. (15b)] was the same as that shown in Eq. (16a). In addition, when the monotonic term  $F_1$  was included in the usual one-step procedure, even greater discrepancies between the real and fitted values of  $\mu$  were observed. However, inclusion of  $F_1$  in the two-step procedure caused essentially no change. Because the values of  $\mu$  obtained from the two-step procedure [using Eqs. (15)] were essentially the same in all three cases, the analysis procedure using the two-step data-reduction method might be more advantageous for experimentalists than the previously used one-step data-reduction analyses.

## V. DISCUSSION

Because of the relatively large difference between the values of the surface reflection coefficient obtained by curve fitting and those obtained by theory<sup>5</sup> (almost 25%), one can speculate on the source of error in the analytical approximations used in the theory.<sup>5</sup> First, Miller and Good have stated that the amplitude of the periodic deviations [see Eq. (8)] in their calculation is low by about 10%, and the phase [see Eq. (10)] is off by less than 3% because of specific approximations in averaging the transmission coefficient  $D(\epsilon, f)$  over the energy  $\epsilon$ . Apart from the stated 10% error, a numerical check of their analytic approximation of the magnitude of the barrier reflection coefficient  $|\lambda|$  [Eq. (14), Ref. 5] shows an additional error estimated to be about 10%.

(These numerical calculations were made for an average energy of 0.01 eV above the top of the barrier and for an average experimental field<sup>2-4</sup> of  $10^5$  V/cm.) This error increases rather sharply with energy; the effective energy bandwidth for the transmission resonance observed in periodic deviations, however, is only about 0.02 eV starting at the barrier maximum, as can easily be seen in Fig. 6 of Ref. 14. The above calculations also show that this error in  $|\lambda|$  increases with decreasing field but is compensated by a smaller interference bandwidth that decreases with decreasing field. Additional error in the analytic expression<sup>5</sup> could be due partially to the assumption that the surface reflection coefficient  $\mu$  is energy-independent and small compared to unity and to the truncation of the transmission coefficient expansion given in Eq. (17):

$$D(\epsilon, f) = (1 - |\lambda|^2)(1 - |\mu|^2)(1 - |\lambda||\mu|^2)^{-1} \\ \times [1 + 2 \sum_{n=1}^{\infty} (-|\lambda\mu|^n \cos n\theta)], \quad (17)$$

where  $\theta = \arg(\lambda^*\mu)$ ,  $\lambda = \lambda(\epsilon, f)$ ,  $\mu = \mu(\epsilon, f)$ . Only the case where  $n=1$  was considered,<sup>5</sup> whereas the  $n=2$  term contributes at least a few percent to  $D(\epsilon, f)$  in the resonance energy region. It appears, therefore, that the 25% discrepancy between the analytic expression and these calculations is quite plausible.

## VI. CONCLUSIONS

In summary, the experimentally observed<sup>3,4</sup> anomalous rise of  $|\mu|$  with field is probably due to real surface potentials that give rise to  $\mu$  reflection coefficients that are more energy-dependent than the  $\mu$  obtained from the box model. The form of the Miller-Good expression [Eqs. (5)-(12)] is valid for the box-model potential. The values of  $|\mu|$  obtained from the expression using least-squares data-reduction methods, however, are approximately 25% too great and the values of  $\arg\mu$  are low by as much as 0.3 rad. Last, most of the corrected estimates of the surface inner potentials  $W_k$  obtained from periodic deviations experiments are now in good agreement with the values calculated from bulk band theory.

## ACKNOWLEDGMENTS

The author is grateful to Dr. G. A. Haas and R. E. Thomas for many stimulating and useful discussions.